is the most important source of the intensity. This was the only term considered by Desjardins et al.[5], but in the present study, all three have been included. An approximate expression for the metal–ligand type integral is given by[34]

$$\langle\psi_i(\mathrm{M})|r_\mu|\phi_j(\mathrm{L})\rangle = \sum_n k_{jn} r_{n\mu}/2\langle\psi_i(\mathrm{M})|\mathrm{p}_n\rangle \qquad (A12)$$

where $r_{nx} = \mathbf{R}\cos\theta_n\cos\alpha_n$, $r_{ny} = \mathbf{R}\cos\theta_n\sin\alpha_n$, $r_{nz} = \mathbf{R}\sin\theta_n$ are operators that rotate the nth p orbital of ligand $\phi_j(\mathrm{L})$. The angles θ_n and α_n describe the position of the nth ligand; θ_n is the angle out of the xy plane and α_n is measured clockwise from the x axis in Figure 1. This then gives an expression of the form

$$\langle\psi_i(\mathrm{M})|r_\mu|\phi_j(\mathrm{L})\rangle = G(\psi_i,\phi_{j'})KR_\mu/2 \qquad (A13)$$

where $R_x = R_y = |\mathbf{R}\cos\theta|$, $R_z = |\mathbf{R}\sin\theta|$ are the magnitudes of the bond length $\mathbf{R}$ in picometers, projected along the molecular axes. Note that $G(\psi_i,\phi_{j'})$ is not necessarily equal to $G(\psi_i,\phi_j)$ because of the sign changes produced by the operator $r_{n\mu}$. $K = 1/2^{1/2}$ if the transition involves an orbital of E symmetry, or K = 1 otherwise.

The ligand–ligand integrals generally involve three centers, but redefining the electronic dipolar operator onto ligand n, $r_\mu = r_{n\mu} + r'_\mu$ gives

$$\langle\phi_i(\mathrm{L})|r_\mu|\phi_j(\mathrm{L})\rangle = \sum_{n,m} k_{in}k_{jm}[r_{n\mu}\langle\mathrm{p}_n|\mathrm{p}_m\rangle + \langle\mathrm{p}_n|r'_\mu|\mathrm{p}_m\rangle] \qquad (A14)$$

The second term in (A14) is now a two-centered integral, which is zero when evaluated by approximation A12, as it has been assumed that there is no ligand–ligand overlap. The form of the expression is then

$$\langle\phi_i(\mathrm{L})|r_\mu|\phi_j(\mathrm{L})\rangle = KR_\mu\langle\phi_i(\mathrm{L})|\phi_j(\mathrm{L})\rangle \qquad (A15)$$

where the symbols have the same meaning as for (A13).

The required expressions for the dipole moments, given as eq 7 in the main text, may now be obtained by substituting the appropriate wave functions (see eq 6 of the main text) into (A11) and making use of (A13) and (A15) above.

Registry No. $(NbzpipzH_2Cl)_2CuCl_4$, 81567-09-1; (Naem)$CuCl_4$, 82621-22-5; Cs_2CuCl_4, 13820-31-0; $CuCl_4^{2-}$, 15489-36-8.

(45) Nelson, H. C.; Simonsen, S. H.; Watt, G. W. *J. Chem. Soc., Chem. Commun.* **1979**, 632.
(46) Larsen, K. P.; Hazell, R. G.; Toftlund, H.; Andersen, P. R.; Bisgard, P.; Edlund, K.; Eliasen, M.; Herskind, C.; Laursen, T.; Pedersen, P. M. *Acta Chem. Scand.* **1975**, *A29*, 499.
(47) Bonamartini, A.; Nardelli, M.; Palmieri, C.; Pelizzi, C. *Acta Crystallogr., Sect. B: Struct. Crystallogr. Cryst. Chem.* **1971**, *B27*, 1775.
(48) Willett, R. D.; Larsen, M. L. *Inorg. Chim. Acta* **1971**, *5*, 175.
(49) Lamotte-Brasseur, J.; Dupont, L.; Dideberg, O. *Acta Crystallogr., Sect. B: Struct. Crystallogr. Cryst. Chem.* **1973**, *B29*, 241.
(50) Bonamico, M.; Dessy, G. *Theor. Chim. Acta* **1967**, *7*, 367.
(51) Clay, R.; Murray-Rust, J.; Murray-Rust, P. *Acta Crystallogr., Sect. B: Struct. Crystallogr. Cryst. Chem.* **1975**, *B31*, 289.

Contribution from the Department of Chemistry, University of Leuven, B-3030 Leuven, Belgium

Weak Field–Strong Field Correlation Diagrams in Transition-Metal Complexes

L. G. Vanquickenborne,* M. Hendrickx, D. Postelmans, I. Hyla-Kryspin, and K. Pierloot

Received July 8, 1987

Ab initio SCF calculations have been performed for two typical Co(III) complexes, viz. CoF_6^{3-} and $Co(CN)_6^{3-}$, not only on their ground state and a selected set of excited states but also on the average of all ligand field states. The frozen orbitals of the latter calculation were used to set up a correlation diagram connecting the free Co(III) ion (weak field side) with all possible $t_{2g}^m e_g^n$ configuration averages for both complexes (strong field side). A comparison of these diagrams with the conventional ligand field picture shows very good qualitative agreement, for instance in characterizing CoF_6^{3-} as a high-spin complex and $Co(CN)_6^{3-}$ as a low-spin complex. Conceptually, however, the interpretation of the diagrams and of the ligand field parameters $10Dq$, B, and C is thoroughly modified by the subtle role of differential covalency and by the influence of shape modifications in the metal d orbitals.

I. Introduction

A key concept in ligand field theory is the Tanabe–Sugano correlation diagram[1] (or the related Orgel diagram[2]), connecting the d^N energy levels at the strong field limit and the weak field limit.[3] If $4 \leq N \leq 7$, the correlation diagram is characterized by a multiplicity change of the ground state, thereby giving rise to the existence of high-spin and low-spin complexes. The classification of a specific compound as high-spin or low-spin is supposed to depend on the relative values of $10Dq$ and P. The one-electron parameter $10Dq$ is a measure of the strength of the ligand field, whereas the spin-pairing parameter P describes the interelectronic d–d repulsion energy.

It is somewhat surprising that correlation diagrams have received so little attention from the ab initio point of view. Indeed, most of the Hartree–Fock calculations on transition-metal complexes have concentrated on other aspects, such as the reproduction of an individual ligand field spectrum, density shifts in the bonding region, bond distances, photoelectron spectra, substitution effects, etc. As a matter of fact, apart from an early study by Kalman and Richardson[4] (using very approximate wave functions) we are aware of only one communication on the subject, where Nieuwpoort[5] compares $FeF_6^{4-,3-}$ and $Fe(CN)_6^{4-,3-}$. Although the author does not discuss correlation diagrams explicitly, he offers an interesting comparison of some of the relevant ligand field energies.

It is the purpose of this paper to present a detailed analysis of the octahedral ligand field levels in the high-spin CoF_6^{3-} and in the low-spin $Co(CN)_6^{3-}$ complexes. Moreover, the basic physical assumptions of ligand field theory will be critically examined in the light of the ab initio wave functions.

II. Method of Calculation

Roothaan's restricted Hartree–Fock scheme[6] for open shells (two Hamiltonian formalism) was used throughout in Sections IV and V. The Roothaan equations have been solved for each specific state, but also for the d^N configuration average. The orbitals of the configuration average were used to recalculate the energies of the individual states. More details on the calculational procedure and on the "frozen orbital calculations" are given in ref 7 and 8.

(1) Tanabe, U.; Sugano, S. *J. Phys. Soc. Jpn.* **1954**, *9*, 753.
(2) Orgel, L. E. *Transition-Metal Chemistry: Ligand-Field Theory*, 2nd ed.; Methuen: London, 1966.
(3) Lever, A. B. P. *Inorganic Electronic Spectroscopy*, 2nd ed.; Elsevier: Amsterdam, 1984.
(4) Kalman, B. L.; Richardson, J. W. *J. Chem. Phys.* **1971**, *55*, 4443.
(5) Nieuwpoort, W. C. *Proceedings of the Fourth Seminar on Computational Methods in Quantum Chemistry*; Max-Planck Institut für Physik und Astrophysik: München, FRG, 1978.
(6) Roothaan, C. C. J. *Rev. Mod. Phys.* **1960**, *32*, 179.
(7) Vanquickenborne, L. G.; Verhulst, J. *J. Am. Chem. Soc.* **1983**, *105*, 1769.

0020-1669/88/1327-0900$01.50/0

Table I. Parentage of the d^6 States in an Octahedral Ligand Field: Left, Weak Field Limit; Right, Strong Field Limit[a]

Co^{3+} zero field	CoF_6^{3-} weak field	$Co(CN)_6^{3-}$ strong field	no repulsion ∞ field
^5D	$^5D_2$, ^5E	$^1A_1$	t_2^6
^3H	^3E, two $^3T_1$, $^3T_2$	$^1T_1$, $^1T_2$, $^3T_1$, $^3T_2$	$t_2^5e^1$
^3G	$^3A_1$, ^3E, $^3T_1$, $^3T_2$	$^5T_2$, $^3A_2$, ^3E, three $^3T_1$, two $^3T_2$, two $^1A_1$, $^1A_2$	$t_2^4e^2$
two ^3F	two $^3A_2$, two $^3T_1$, two $^3T_2$	three ^1E, $^1T_1$, three $^1T_2$	
^3D	$^3T_2$, ^3E	^5E, $^3A_1$, $^3A_2$, two ^3E, two $^3T_1$, two $^3T_2$, $^1A_1$	$t_2^3e^3$
two ^3P	two $^3T_1$	$^1A_2$, ^1E, two $^1T_1$, two $^1T_2$	
^1I	$^1A_1$, $^1A_2$, ^1E, $^1T_1$, two $^1T_2$	$^3T_1$, $^1A_1$, ^1E, $^1T_2$	$t_2^2e^4$
two ^1G	two $^1A_1$, two ^1E, two $^1T_1$, two $^1T_2$		
^1F	$^1A_2$, $^1T_1$, $^1T_2$		
two ^1D	two $^1T_2$, two ^1E		
two ^1S	two $^1A_1$		

[a] The ground states are in boldface. The subscript g has been dropped everywhere.

The geometry of the two complexes was taken to be strictly octahedral at the experimental bond lengths,[9-11] that is, with the Co–F distance equal to 1.89 Å, the Co–C distance equal to 1.89 Å, and the C-N distance equal to 1.15 Å. The metal basis set was taken as (15s 11p 6d/11s 8p 4d)—as detailed elsewhere[7-8]—and the ligands were described by the Huzinaga–Dunning[12,13] basis set (9s 5p/5s 3p).

III. Ligand Field Analysis of the Experimental Data

It is well-known that nearly all octahedral Co(III) complexes are diamagnetic; they are characterized by a low-spin ground state. It is obvious that also the very strong cyanide ligand will give rise to a $^1A_{1g}(t_{2g}^6)$ ground state. CoF_6^{3-} on the other hand is one of the few known high-spin Co(III) complexes, characterized by a paramagnetic $^5T_{2g}(t_{2g}^4e_g^2)$ ground state.[14]

Table I recalls the parentage of the different possible octahedral d^6 states in both the strong and the weak field limits. Only a few of the 43 possible states are observed and assigned. Only three out of these 43 states are unique ($^5T_2$, ^5E, and $^3A_1$); the other 40 states will to some extent be affected by configuration interaction within the d^6 manifold.

The available experimental data[14-16] are listed in Table II, together with the assignments proposed on the basis of ligand field calculations.[15,16] The empirical ligand parameters $10Dq$, B, and C, deduced on the basis of Table II, are 14 100 cm^{-1}, 765 cm^{-1}, and 3672 cm^{-1} for the fluoride complex[15] and 34 890 cm^{-1}, 448 cm^{-1}, and 3548 cm^{-1} for the cyanide complex.[16,17]

Obviously, CoF_6^{3-} is a typical weak field complex, whereas $Co(CN)_6^{3-}$ is definitely a strong field complex; the ratio of the two Dq values is ≃2.5. Tanabe and Sugano predicted[1] the singlet–quintet crossover to take place at $10Dq/B \simeq 20$. From Table II, the actual value of $10Dq/B$ is found to be 18 for the fluoride and 78 for the cyanide complex. The Racah parameters (especially B) are smaller for $Co(CN)_6^{3-}$ than for CoF_6^{3-}, indicating a larger nephelauxetic effect—and a correspondingly larger covalency—for the cyanide complex. The spin-pairing energy[18,19] exceeds the spectrochemical strength for CoF_6^{3-}, but not for $Co(CN)_6^{3-}$.

In the fluoride complex, one of the observed transitions ($^5T_{2g} \rightarrow {}^5E_g$) corresponds exactly to $10Dq$, since ligand field theory predicts the same d–d repulsion energy for both states. In the cyanide complex, this transition is of course not observable, and all the observed transitions depend both on Dq and on the Racah parameters. For instance, the $^1A_{1g}(t^6) \rightarrow {}^1T_{1g}(t^5e^1)$ transition is at $10Dq - C$, while the $^1A_{1g}(t^6) \rightarrow {}^1T_{2g}(t^5e^1)$ transition is at $10Dq - C + 16B$, giving rise to an energy gap of $16B$; the corresponding triplets are separated by an energy gap of only $8B$.

IV. Frozen Orbital Calculations

A. Average Electrostatic Field. A single configuration Hartree–Fock calculation yields slightly different orbitals for each one of the possible states corresponding to a given d^N or $t_{2g}^m e_g^n$ configuration ($n + m = N$). It is possible, however, to carry out a single Hartree–Fock calculation for the molecular d^N system, i.e. the weighted average of all possible ligand field states. Using the resulting (frozen) orbitals, one can then obtain a (somewhat less accurate) description of any given multiplet belonging to the set under consideration.

If this frozen orbital approach is used for transition metal atoms or atomic ions, the valence repulsion of all states resulting from one given d^N configuration can be described by means of only three Racah parameters, A, B, and C. The simplicity of this parametrization scheme goes back to the 5-fold degeneracy of the d orbitals, which are characterized by one common radial part. Conventional multiplet theory makes use of the frozen orbital approximation, although the analytical calculation of the d orbitals is not always explicity carried out. Still, the energy expressions for the different states are parametrized in terms of one common set of frozen orbitals.[19,20]

Ligand field theory, being a perturbational approach, builds on the same basis and describes the different repulsion effects—also in *molecular* complexes—by the same three atomic Racah parameters. Yet, in a $t_{2g}^m e_g^n$ configuration—even in a frozen orbital approximation—there are in principle *two different* radial wave functions. In the interpretation of ligand field spectra, this difference between e_g and t_{2g} shells has to some extent been recognized and has led to the introduction of Racah parameters, specific for the different subshells.[3] A more refined treatment of molecular complexes, fully accounting for the different radial wave functions of the t_{2g} and the e_g orbitals, requires the use of ten Griffith parameters[19] (to replace the three atomic Racah parameters). The connection between the two sets of parameters is given in Table III. Generally, in the interpretation of experimental spectra, the use of the Griffith parameters is not appropriate, since the number of available spectral transitions is often much less than 10. But from the present point of view, it appears to be indicated to use one and the same set of frozen orbitals (calculated from the appropriate Hartree–Fock equation for the d^N system) and to use the corresponding Griffith parameters to derive the frozen orbital energies of the relevant states and the corresponding $t_{2g}^m e_g^n$ averages. These results can then be compared on the one hand with ligand field theory (which is a more simplified version of a frozen orbital calculation) and, on the other hand, with the Hartree–Fock calculations on the individual states. The molecular frozen orbital calculations apparently offer a convenient meeting point between these two rather different treatments.

B. Correlation Diagrams. Figures 1 and 2 show the Hartree–Fock correlation diagrams for CoF_6^{3-} and $Co(CN)_6^{3-}$. At the right-hand side of both diagrams, the Co^{3+} free ion energies

(8) Vanquickenborne, L. G.; Haspeslagh, L.; Hendrickx, M.; Verhulst, J. *Inorg. Chem.* **1984**, *23*, 1677.
(9) Hepworth, M. A.; Jack, K. H.; Peacock, R. O.; Westland, G. J. *Acta Crystallogr.* **1957**, *10*, 63.
(10) Vannerberg, N. G. *Chem. Scr.* **1976**, *9*, 22.
(11) Iwata, M.; Saito, Y. *Acta Crystallogr., Sect. B: Struct. Crystallogr. Cryst. Chem.* **1973**, *B29*, 822.
(12) Dunning, T. H. *J. Chem. Phys.* **1970**, *53*, 2823.
(13) Huzinaga, S. *J. Chem. Phys.* **1965**, *42*, 1293.
(14) Cotton, F. A.; Meyer, M. D. *J. Am. Chem. Soc.* **1960**, *82*, 5023.
(15) Allen, G. C.; El-Sharkawy, G. A. M.; Warren, K. D. *Inorg. Chem.* **1971**, *10*, 2538.
(16) Viaene, L.; D'Olieslager, J.; Ceulemans, A.; Vanquickenborne, L. G. *J. Am. Chem. Soc.* **1979**, *101*, 1405.
(17) Vanquickenborne, L. G.; Hendrickx, M.; Hyla-Kryspin, I.; Haspeslagh, L. *Inorg. Chem.* **1986**, *25*, 885.
(18) Vanquickenborne, L. G.; Haspeslagh, L. *Inorg. Chem.* **1982**, *21*, 2448.
(19) Griffith, J. S. *The Theory of Transition Metal Ions*; Cambridge University Press: London, 1971.
(20) Slater, J. C. *Quantum Theory of Atomic Structure*; McGraw-Hill: New York, 1960; Vol. I and II.

(21) In eq 16a and Table VI, the notation $C_0(^1A_1)$ is the repulsion associated with the closed t_{2g}^6 shell. The subscript refers to the Hartree–Fock equation of the d^6 configuration average, whose solution yields the open-shell t_{2g} orbitals that are used in the calculation of the $^1A_1$ state.

Table II. Assignment[a] of the Experimental Ligand Field Spectra of CoF_6^{3-} and $Co(CN)_6^{3-}$ [15,16]

band max for CoF_6^{3-}, $cm^{-1} \times 10^3$	assignt[b]	band max for $Co(CN)_6^{3-}$, $cm^{-1} \times 10^3$	assignt
5.5	$^5T_{2g}(t^4e^2) \rightarrow {}^3T_{1g}(t^5e^1)$	25.2	$^1A_{1g}(t^6) \rightarrow {}^3T_{1g}(t^5e^1)$
11.8, 16.4	$\rightarrow {}^5E_g(t^3e^3)$[c]	32.5	$\rightarrow {}^1T_{1g}(t^5e^1)$
19.6	$\rightarrow {}^3T_{1g}(t^4e^2)$ $\rightarrow {}^3T_{2g}(t^4e^2)$	39.2	$\rightarrow {}^1T_{2g}(t^5e^1)$
23.3	$\rightarrow {}^3E_g(t^4e^2)$ $\rightarrow {}^3T_{1g}(t^4e^2)$		
26.3	$\rightarrow {}^3T_{2g}(t^4e^2)$		
30.3	$\rightarrow {}^3A_{2g}(?)(t^3e^3)$		

[a] The corresponding ligand field parameters $10Dq$, B, and C are 14 100 cm^{-1}, 765 cm^{-1}, and 3672 cm^{-1} for CoF_6^{3-} and 34 890 cm^{-1}, 448 cm^{-1}, and 3548 cm^{-1} for $Co(CN)_6^{3-}$. [b] Also for the fluoride complex, the strong field parentage is shown in parentheses, as this was the labeling preferred by Allen et al.;[15] the connection with the weak field labels is unambiguous. [c] Due to a tetragonal Jahn–Teller distortion of the ^5E_g level, the corresponding transition is split into two bands, the average being taken as $10Dq$.

Table III. Griffith and Racah Parameters as a Function of Certain J and K Integrals[a]

$a = J_{\xi\xi} = J_{\eta\eta} = J_{\zeta\zeta}$	$A + 4B + 3C$
$b = J_{\xi\eta} = J_{\xi\zeta} = J_{\eta\zeta}$	$A - 2B + C$
$j = K_{\xi\eta} = K_{\xi\zeta} = K_{\eta\zeta}$	$3B + C$
$e = J_{\theta\theta} = J_{\epsilon\epsilon}$	$A + 4B + 3C$
$f = K_{\theta\epsilon}$	$4B + C$
$c = (3^{1/2}/2)(J_{\theta\xi} - J_{\epsilon\xi}) = (3^{1/2}/2)(J_{\theta\eta} - J_{\epsilon\eta})$	$2(3^{1/2})B$
$d = J_{\epsilon\xi} = J_{\epsilon\eta}$	$A - 2B + C$
$g = K_{\theta\xi} = K_{\epsilon\eta}$	$B + C$
$h = (3^{1/2}/2)(K_{\epsilon\xi} - K_{\theta\xi}) = (3^{1/2}/2)(K_{\epsilon\eta} - K_{\theta\eta})$	$3^{1/2}B$
$f - j$	B
$K_{\epsilon\zeta}$	C

[a] In the atomic case, the 10 Griffith parameters become linearly dependent and can be expressed as a function of the three Racah parameters: a becomes equal to $A + 4B + 3C$, and also $a - b = 2j$, etc. As usual,[19] θ and ϵ are the two e_g orbitals, transforming like z^2 and $x^2 - y^2$, respectively, ξ, η, and ζ are the three t_{2g} orbitals, transforming like yz, xz, and xy, respectively.

were calculated from the frozen orbitals of the $3d^6$ average; in the remainder of the figures, the state energies and the energies of the $t_{2g}^m e_g^n$ averages were calculated from the frozen orbitals of the d^6 average for CoF_6^{3-} (Figure 1) and $Co(CN)_6^{3-}$ (Figure 2).

The most striking feature of Figures 1 and 2 is the unambiguous classification of CoF_6^{3-} as a high-spin complex and $Co(CN)_6^{3-}$ as a low-spin complex. The fact that the correct ground states are reproduced at the Hartree–Fock level of approximation is not trivial. Indeed, it is well-known that the high-spin quintet states incorporate the Pauli correlation and are therefore expected to be described significantly better at the Hartree–Fock level than the low-spin singlet states. Obviously, this differential correlation effect does not prevent the Hartree–Fock calculations from predicting the correct ground state in both cases, even in the frozen orbital approximation.

A comparison of Figures 1 and 2 also clearly reveals that the molecular $t_2^m e^n$ energy splittings (left-hand side of both diagrams) are much smaller in the hexafluoride complex than in the hexacyanide complex.

1. $t_{2g}^m e_g^n$ Configurations. Obviously, Figures 1 and 2 are not quite identical with the correlation diagrams of ligand field theory: at the left-hand side of both figures, the repulsion effects are not negligibly small with respect to the one-electron energy differences. Still, as the $t_{2g}^m e_g^n$ levels are not split by electron repulsion effects, they represent the closest approach of the Hartree–Fock method to the strong field limit.

In a conventional ligand field correlation diagram, the strong field $t_{2g}^m e_g^n$ configurations are separated by a constant energy interval, viz. $10Dq$. This is obviously not the case in Figures 1 and 2. As a matter of fact, the energy separation between two subsequent configurations

$$\Delta E_m^{m-1} = E(t_{2g}^{m-1} e_g^{n+1}) - E(t_{2g}^m e_g^n)$$

shows a strictly linear increase with decreasing m. The origin of this linear dependence can readily be understood from a detailed analysis of the $t_{2g}^m e_g^n$ energy expression:

$$E(t_{2g}^m e_g^n) = E_c + L_o + T_o + C_{oc} + C_o \quad (1)$$

The first four terms in this equation are identical for all states corresponding to the $t_{2g}^m e_g^n$ configuration. E_c is the energy contribution of the closed shells, which is independent of m or n, L_o and T_o are the electron–nuclear attraction and the kinetic energy of the open shells, respectively, and C_{oc} is the repulsion between the open and the closed shells. The last term, C_o, represents the average open-shell repulsion energy for the $t_{2g}^m e_g^n$ states.

A more explicit expression for C_o is given by[20]

$$C_o(t_{2g}^m e_g^n) = \tfrac{1}{2}m(m-1)\bar{C}_{tt} + \tfrac{1}{2}n(n-1)\bar{C}_{ee} + mn\bar{C}_{te} \quad (2)$$

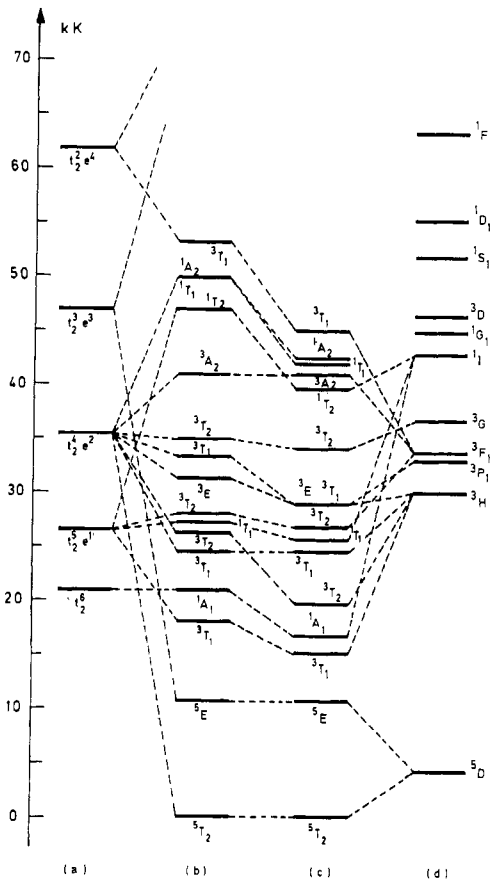

Figure 1. Correlation diagram of CoF_6^{3-} based on frozen orbital Hartree–Fock calculations. Apart from the energies of the $t_2^m e^n$ configuration averages (a) and the individual states (b), the diagram also shows the results of configuration interaction with the ligand field states (LFCI) (c). The right-hand side of the figure (d) shows the energy levels of the atomic Co^{3+} ion.

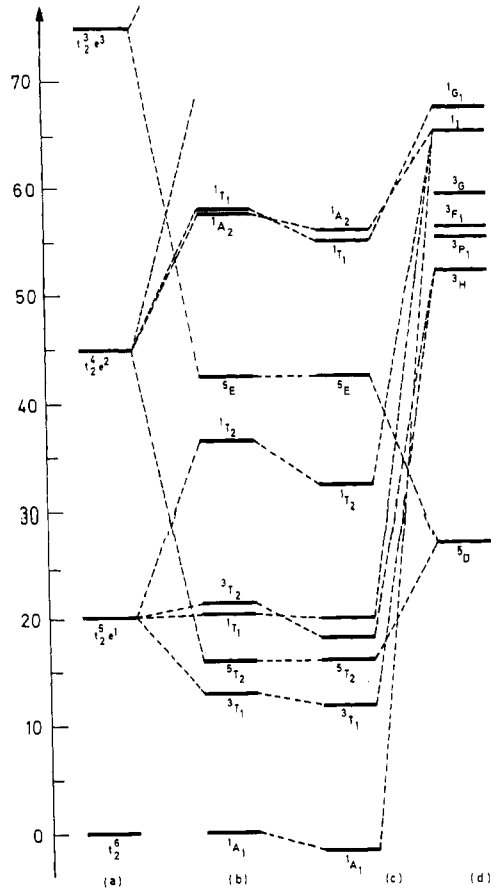

Figure 2. Correlation diagram of $Co(CN)_6^{3-}$ based on frozen orbital Hartree–Fock calculations. Apart from the energies of the $t_2^m e^n$ configurations averages (a) and the individual states (b), the diagram also shows the results of configuration interaction with the ligand field states (LFCI) (c). The right-hand side of the figure (d) shows the energy levels of the atomic Co^{3+} ion.

where $\bar{C}_{tt}$ and $\bar{C}_{ee}$ represent the average repulsion between two electrons in the t_{2g} and e_g shells, respectively, while $\bar{C}_{te}$ stands for the average repulsion between an electron in the t_{2g} shell and an electron in the e_g shell.

The quantities $\bar{C}_{tt}$, $\bar{C}_{ee}$, and $\bar{C}_{te}$ can further be detailed by using the following simple but general expression for the two shells λ and μ

$$\bar{C}_{\lambda\mu} = \frac{1}{M}\sum_{p=1}^{d_\lambda}\sum_{q=1}^{d_\mu}(2J_{pq} - K_{pq}) \tag{3}$$

where the summation runs over the space orbitals, d_λ and d_μ stand for the spatial degeneracies of the λ and μ shells, and M is proportional to the number of different two-electron interactions

$$M = 2d_\lambda d_\mu \quad \text{when } \lambda \neq \mu$$

$$M = d_\lambda(2d_\lambda - 1) \quad \text{when } \lambda = \mu$$

When the relevant Coulomb and exchange integrals are replaced by the appropriate Griffith parameters (see Table III), one obtains

$$\bar{C}_{tt} = \frac{1}{5}(a + 4b - 2j)$$

$$\bar{C}_{ee} = e - \frac{5}{3}f \tag{4}$$

$$\bar{C}_{te} = d + \frac{c}{3^{1/2}} - \frac{1}{2}g - \frac{1}{2(3^{1/2})}h$$

The values of the Griffith parameters for the CoF_6^{3-} and $Co(CN)_6^{3-}$ complex are given in Table IV, together with the corresponding values of $\bar{C}_{tt}$, $\bar{C}_{ee}$, and $\bar{C}_{te}$.

Table IV. Griffith Parameters (in hartrees) Determined from Frozen Orbital SCF Calculations on the d^6 Configuration Average of Co^{3+}, CoF_6^{3-} (Corresponding to Figure 1), and $Co(CN)_6^{3-}$ (Corresponding to Figure 2)[a]

	Co^{3+}	CoF_6^{3-}	$Co(CN)_6^{3-}$
a	1.054 034	0.999 133	0.946 369
b	0.970 462	0.920 995	0.873 442
c	0.021 518	0.019 616	0.016 483
d	0.970 462	0.897 184	0.786 249
e	1.054 034	0.949 011	0.770 963
f	0.047 998	0.042 670	0.033 238
g	0.029 362	0.026 420	0.021 322
h	0.010 759	0.009 680	0.007 787
i	0.010 759	0.009 852	0.008 510
j	0.041 786	0.039 045	0.036 489
$\bar{C}_{tt}$	0.970 462	0.921 005	0.873 432
$\bar{C}_{ee}$	0.974 037	0.877 894	0.715 566
$\bar{C}_{te}$	0.965 099	0.892 505	0.782 857
$\bar{C}_{tt} + \bar{C}_{ee} - 2\bar{C}_{te}$	3139	3048	5110
$\bar{C}_{tt} - \bar{C}_{te}$	1177	6255	19878
$\bar{C}_{ee} - \bar{C}_{te}$	1962	−3207	−14768

[a] The $\bar{C}_{tt}$, $\bar{C}_{ee}$, and $\bar{C}_{te}$ parameters are linear combinations of the Griffith parameters defined in eq 4. The energies of the three bottom lines are in cm^{-1}.

For any $t_{2g}^m e_g^n$ configuration, $n = N - m$, and for one specific value of N, eq 2 is a parabolic function of m. Therefore, the difference in open-shell repulsion between two successive $t_{2g}^m e_g^n$ configurations is linearly dependent on m:

$$(\Delta C_o)_m^{m-1} = C_o(t_{2g}^{m-1}e_g^{n+1}) - C_o(t_{2g}^m e_g^n)$$
$$= N(\bar{C}_{ee} - \bar{C}_{te}) + (\bar{C}_{tt} - \bar{C}_{te}) - m(\bar{C}_{tt} + \bar{C}_{ee} - 2\bar{C}_{te}) \tag{5}$$

In the expression of the *total* energy difference

$$\Delta E_m^{m-1} = (\Delta L_o + \Delta T_o + \Delta C_{oc} + \Delta C_o)_m^{m-1} \tag{6}$$

the open-shell repulsion term $(\Delta C_o)_m^{m-1}$ is responsible for the linear increase of ΔE with decreasing m (Figures 1 and 2). The first three terms are independent of m. They can be taken together as

$$\Delta E_m^{m-1} = 10Dq(\mathrm{FO}) + (\Delta C_o)_m^{m-1} \tag{7}$$

where FO stands for frozen orbitals and

$$10Dq(\mathrm{FO}) = (\Delta L_o + \Delta T_o + \Delta C_{oc})_m^{m-1} \tag{8}$$

$10Dq$(FO) denotes the frozen orbital MO analogue of the one-electron crystal field parameters $10Dq$: it contains all the energy contributions of ΔE_m^{m-1} except for the open-shell repulsion. Numerically, its value amounts to 36 910 cm^{-1} for CoF_6^{3-} and 119 245 cm^{-1} for $Co(CN)_6^{3-}$ (see also Table V). These values—while showing the expected trend, with $10Dq$(FO) for CoF_6^{3-} being smaller than that for $Co(CN)_6^{3-}$—are very large when compared to the experimental values of $10Dq$ (see Table II).

Both theoretical quantities, $10Dq$(FO) and $(\Delta C_o)_m^{m-1}$, will now be discussed in some detail.

2. Electron Repulsion Parameters. Equation 7 shows that the value of $(\Delta C_o)_m^{m-1}$ determines the difference between ΔE_m^{m-1} and $10Dq$(FO). Clearly, $(\Delta C_o)m^{m-1}$ has to be large and negative. This can easily be verified from eq 5, and by substituting the appropriate values from Table V, one obtains (in cm^{-1}) for CoF_6^{3-}

$$(\Delta C_o)_m^{m-1} = -12\,987 - 3048m \tag{9}$$

and for $Co(CN)_6^{3-}$

$$(\Delta C_o)_m^{m-1} = -68\,730 - 5110m \tag{10}$$

In other words, $(\Delta C_o)_m^{m-1}$ takes on large negative values for all possible values of m. Obviously, the open-shell repulsion strongly favors the occupation of the e_g shell. The effect is definitely more pronounced for $Co(CN)_6^{3-}$ than for CoF_6^{3-}. Moreover, $(\Delta C_o)_m^{m-1}$ becomes less negative as the e_g population increases—resulting

Table V. Three Different Parametrization Schemes, Each Characterized by a "Spectrochemical Strength" and a Corresponding Set of "Repulsion Parameters" (All in cm^{-1})[a]

	Co^{3+}	CoF_6^{3-}	$Co(CN)_6^{3-}$
B	1065	765	448
C	5120	3672	3548
$10Dq$		14100	34890
B_{SCF}	1363	1245	997
C_{SCF}	5081	4593	3560
$10Dq_{SCF}$		10590	26602
$10Dq$(FO)		36910	119245
ΔC_o		−26320	−92624
ΔL		40619	570865
ΔT		72587	658
ΔC_∞		−76296	−452278

[a] $10Dq$, B, and C are the semiempirical parameters reproducing the experimental spectra (Table II). $10Dq_{SCF}$ is the calculated ^5E–$^5T_2$ energy gap at the frozen orbital SCF level. B_{SCF} and C_{SCF} are theoretical parameters obtained from a least-squares fit of the frozen orbital SCF calculations to the ligand field expression. $10Dq$(FO) and ΔC_o are defined in eq 7, 8, 14, and 15. Obviously $10Dq_{SCF} = 10Dq(FO) + \Delta C_o$.

in the linear increase of ΔE_m^{m-1} with decreasing m (see Figures 1 and 2).

Equation 5 and Table IV show that the negative value of $(\Delta C_o)_m^{m-1}$ can be traced back to the relative magnitude of the different open-shell repulsion components

$$\bar{C}_{ee} < \bar{C}_{te} < \bar{C}_{tt}$$

The dominant term is $(\bar{C}_{ee} - \bar{C}_{te})$, which is negative and enters the expression of $(\Delta C_o)_m^{m-1}$ with a factor $N = 6$.

It is instructive to compare this situation with the case of atomic metal ions. Here, the Griffith parameters are not linearly independent (e.g. $a = e$, $a - b = 2j$, etc.) and (3) can be expressed[20] in terms of the three Racah parameters, A, B, and C.

$$\begin{aligned} \bar{C}_{tt} &\rightarrow A - 2B + C = A + D \\ \bar{C}_{ee} &\rightarrow A - (8/3)B + (4/3)C = A + (4/3)D \\ \bar{C}_{te} &\rightarrow A - B + (1/2)C = A + (1/2)D \end{aligned} \qquad (11)$$

where $D = C - 2B$. In all known cases, the semiempirical value of $C > 2B > 0$, and $D > 0$. Therefore, on the basis of conventional multiplet theory, one expects for atomic ions

$$\bar{C}_{ee} > \bar{C}_{tt} > \bar{C}_{te}$$

The value of the Griffith parameters, $\bar{C}_{tt}$, $\bar{C}_{ee}$, and $\bar{C}_{te}$ and their relevant combinations for the Co^{3+} ion are also given in Table IV. $(\bar{C}_{tt} - \bar{C}_{te})$ and $(\bar{C}_{ee} - \bar{C}_{te})$ are now both positive, and so is the constant term in eq 5. For Co^{3+}, one obtains (in cm^{-1})

$$(\Delta C_o)_m^{m-1} = 1249 - 3139m \qquad (12)$$

This means that now $(\Delta C_o)_m^{m-1}$ is negative for large m values and becomes positive for smaller m. In other words, the parabola of eq 2 has a minimum within the range of accessible m values. This result is to be expected on general grounds: in atoms the interelectronic repulsion will be minimized if the electrons are distributed over the t_{2g} *and* the e_g orbitals, rather than if they are clustered together either in the t_{2g} *or* in the e_g orbitals.

As stressed before, the situation is entirely different in molecular complexes. Indeed, Table IV shows how the repulsion integrals all decrease from Co^{3+} to CoF_6^{3-} to $Co(CN)_6^{3-}$. This is of course directly related to the fact that the atomic d orbitals are replaced by more delocalized molecular orbitals and that the cyanide complex is more covalent than the fluoride complex (nephelauxetic effect). From Table IV it is also clear that the molecular e_g orbitals carry significantly less repulsion than the t_{2g} orbitals. This is related to the more covalent and therefore more delocalized nature of the e_g dσ orbitals. These observations are entirely consistent with an analysis of the metal d character of the open-shell orbitals.[8] The differential covalency between the e_g and t_{2g} orbitals is clearly more pronounced in the cyanide than in the fluoride complex. These trends are all seen to be reflected in eq 9 and 10.

On the other hand, if one considers the energy difference between two states within the *same* configuration, ΔC_o can obviously not be affected by differential covalency. For example, the strong field energies for $^1A_2(t_2^4e^2)$ and $^1T_1(t_2^4e^2)$ are identical in Racah's parametrization scheme; in the molecular case, their energy difference equals $a - b - 2j$, which amounts to 11 cm^{-1} for CoF_6^{3-} and to −11 cm^{-1} for $Co(CN)_6^{3-}$. The two states are therefore effectively degenerate. The fact that the atomic relationship $(a - b = 2j)$ is very nearly satisfied, is an indication of the small covalency and the almost purely atomic d character of the open-shell t_{2g} orbitals.

3. Spectrochemical Strength. In crystal field theory, the energy difference between ^5E_g and $^5T_{2g}$ is set equal to $10Dq$: since both states have the same ^5D parentage and since ^5D is the only quintet within the d^6-configuration, crystal field theory associates the same open-shell repulsion with both states. In molecular orbital theory, however, the open-shell repulsion

$$\Delta C_o = C_o(^5E;t^3e^3) - C_o(^5T_2;t^4e^2) = d + 2e - a - 2b + c/3^{1/2} - 2f \qquad (13)$$

is definitely not zero; it amounts to −26 320 cm^{-1} for CoF_6^{3-} and to −92 624 cm^{-1} for $Co(CN)_6^{3-}$ (see Tables IV and V). The magnitude of these numbers is a measure of the conceptual difference between crystal field theory and the best possible single-configuration frozen orbital picture for the complexes under consideration. The excited ^5E state carries much less open-shell repulsion than the lower lying $^5T_2$ state, essentially because of the more covalent character of the e_g dσ orbitals.

The total energy difference is given by

$$\Delta E = E(^5E;t^3e^3) - E(^5T_2;t^4e^2) = 10Dq(FO) + \Delta C_o \qquad (14)$$

where $10Dq$(FO) is defined in eq 8. ΔE itself can be considered as the theoretical value of the spectrochemical strength, since it corresponds to the ^5E–$^5T_2$ energy gap ($10Dq$ in crystal field analysis). Therefore, ΔE may also be denoted as $10Dq_{SCF}$ and

$$\Delta E = 10Dq_{SCF} = 10Dq(FO) + \Delta C_o \qquad (15)$$

The numerical value of $10Dq_{SCF}$ equals 10 590 cm^{-1} for CoF_6^{3-} and 26 602 cm^{-1} for $Co(CN)_6^{3-}$ (see also Table V).

A decomposition of $\Delta E = 10Dq_{SCF}$ into its components is given in Table V where the excitation energy is seen to be the result of a cancellation of very large contributions. The $t_{2g} \rightarrow e_g$ excitation apparently corresponds to a decrease of both $\bar{C}_\infty$ and $|L|$. Both phenomena are due to the larger covalency of the e_g orbitals reducing the interaction of the open-shell electrons with both the metal nucleus and the electron core.

ΔT is by itself the result of two opposing effects: the larger mixing of ligand character into the cobalt d_σ orbitals increases the orbital size and therefore tends to reduce the kinetic energy. Simultaneously, however, the strong antibonding nature of this mixing induces steep gradients in the wave functions, which tend to make ΔT positive. Table V indicates that the latter effect is dominant in CoF_6^{3-}, whereas in $Co(CN)_6^{3-}$ both effects very nearly cancel and ΔT is very small.

Obviously, the energy component analysis leads to a physical picture that is very different from the conventional ligand field ideas, where the differential covalency between e and t_2 orbitals is completely neglected, and where $\Delta T = 0$. Even for $Co(CN)_6^{3-}$, where ΔT is (accidently) found to be very small, the large negative value of ΔC_o (−92 624 cm^{-1}) shows to what extent the SCF description is different from the crystal field picture.

In view of these facts, it is intriguing that—for both complexes—the ligand field expressions do provide a good description of the experimental spectra: the empirical ligand field parameters $10Dq$, B, and C of Table II (which are also resumed in Table V) reproduce the observed bands quite satisfactorily. Although $10Dq$ and $10Dq_{SCF}$ are of the same order of magnitude, the latter quantity is seen to result from the partial cancellation of two large quantities: $10Dq(FO) >> 0$ and $\Delta C_o << 0$. As a consequence, $10Dq$(FO) is much larger than $10Dq$ or $10Dq_{SCF}$,

Table VI. Energy Difference between the Lowest Singlet and the Lowest Quintet of Co^{3+}, CoF_6^{3-}, and $Co(CN)_6^{3-}$ As Determined from a Frozen Orbital SCF Calculation on the d^6 Configuration Average[a]

	Co^{3+}	CoF_6^{3-}	$Co(CN)_6^{3-}$
ΔE	38 921	20 789	15 746
ΔC_o	38 921	94 609	222 744
ΔC_∞	0	152 592	904 556
ΔC	38 921	247 201	1127 300
ΔL	0	−81 238	−1141 730
ΔT	0	−145 174	−1 316
$-20Dq$(FO)		−73 820	−238 490
$-20Dq_{SCF}$		21 180	53 204
$5B_{SCF} + 8C_{SCF}$		42 969	33 465

[a] The energy components are defined in eq 1 and 8, $\Delta E = E$(singlet) $- E$(quintet). All energies are in cm^{-1}. The parameters B_{SCF} and C_{SCF} are determined from a least-squares fit of the SCF results to the crystal field expressions; they do not, therefore, reproduce ΔE exactly.

but the ratio of the spectrochemical strength of the fluoride and cyanide complex is comparable for the three Dq parameters.

4. Ground-State Description and Singlet–Quintet Balance. The energy difference between the two possible ground states in the frozen orbital approximation is given by the MO expression[22]

$$E(^1A_1) - E(^5T_2) = -20Dq(FO) + C_o(^1A_1) - C_o(^5T_2) = -20Dq(FO) + 2a + 7b - (8/3^{1/2})c - 8d - e + 3f + 6g + (6/3^{1/2})h - 3j \quad (16a)$$

or alternatively by the crystal field expression

$$E(^1A_1) - E(^5T_2) = -20Dq + 5B + 8C \quad (16b)$$

where $5B + 8C$ represents the crystal field pairing energy.

Table VI shows the numerical value of the relevant quantities. As stressed before, the SCF calculations predict the correct ground state in both cases: ΔE is positive for CoF_6^{3-} and negative for $Co(CN)_6^{3-}$. The open-shell repulsion is larger in the singlet state than in the quintet state for two reasons, first because filling up the t_{2g} shell (by pairing the electrons) requires more energy than having two electrons in the e_g shell with parallel spins and second because the t_{2g} shell is more ionic and therefore more compact. The first effect is the only one that is operative in atomic ions (see the Co^{3+} column of Table VI). The latter effect, which is neglected in the classical picture, is quite important, since ΔC_o is larger for $Co(CN)_6^{3-}$ than for CoF_6^{3-} (222.7 versus 94.6 × 10^3 cm^{-1}), although the Griffith parameters of the cyanide complex are the *smaller* ones.[22]

Obviously, it is the *differential* covalency of the e_g and the t_{2g} orbitals that results in ΔC_o being larger for the cyanide complex. As was shown in the previous section, the same factor is also largely responsible for $10Dq$(FO) being larger for the cyanide complex. Both terms tend to cancel in the total energy expression (eq 16).

Here, as in the previous section, this cancellation seems to be the main reason that ligand field theory is not an altogether unreasonable parametrization scheme. Ligand field theory does not account for the differential covalency of the $d\sigma$ and $d\pi$ orbitals; it assigns the open-shell repulsion differences entirely to the classical spin pairing energy. Focusing on just one of the physical differences between singlet and quintet state (albeit the smaller one) is a convenient way to take advantage of the partial cancellation of the two terms under consideration. The price one has to pay is that now the open-shell repulsion difference *appears* to be the smaller one in $Co(CN)_6^{3-}$ (33.5 versus 43.0 × 10^3 cm^{-1} in CoF_6^{3-}).

C. LFCI and Comparison with Experiment. In conventional ligand field theory, the most satisfactory description of a transition-metal complex is not limited to a strong field or a weak field treatment only, but instead one diagonalizes the complete ligand field matrix. In the frozen orbital SCF framework, this corresponds to a ligand field configuration interaction (LFCI) treatment. The results of an LFCI calculation for CoF_6^{3-} and $Co(CN)_6^{3-}$ are shown in the middle of Figures 1 and 2. This is as far as one can go in the frozen orbital approximation of d^6 systems.[23] To the extent that a comparison with experimental data is available, it is clear that the qualitative features of both CoF_6^{3-} and $Co(CN)_6^{3-}$ are reproduced very satisfactorily. Quantitatively however, the intraconfigurational transitions are calculated too high. As for the interconfigurational transitions, the $t_{2g} \rightarrow e_g$ promotions are predicted too small and the $e_g \rightarrow t_{2g}$ transitions are calculated too high. One consequence is that the energy levels of $^3T_{1g}(t_{2g}^5e_g^1)$ and $^5E_g(t_{2g}^3e_g^3)$ in Figure 1 are inverted with respect to the experimental data. Table V compares the semiempirical and theoretical ligand field parameters: B_{SCF} and C_{SCF} are seen to vary in the observed direction, but quantitatively they remain too large. This is a well-known phenomenon, which is related to the fact that the intra d^n transitions are calculated too high even in the free atomic ion. The relative energies are very well reproduced, but the calculated energy gaps are some 15% larger than the observed transitions.

Similarly, the calculated $10Dq$ values ($t_{2g} \rightarrow e_g$ transitions) are of the correct order of magnitude and even of the correct relative value

$$\frac{10Dq_{SCF}(Co(CN)_6^{3-})}{10Dq_{SCF}(CoF_6^{3-})} \simeq 2.5 \simeq \frac{10Dq(Co(CN)_6^{3-})}{10Dq(CoF_6^{3-})}$$

but the numerical values are some 25% too low. It is well-known that a much more elaborated treatment of electron correlation is necessary to remedy these remaining discrepancies.[24,25]

V. Hartree–Fock Calculations for the Individual States

1. Relaxation Energies. Within the framework of the Hartree–Fock approach, the most obvious refinement consists in carrying out complete SCF calculations for each individual state, rather than using one common frozen orbital set for all d^N terms. The energy improvement obtained in this way corresponds to the change in the wave function, when the orbitals relax from the frozen set to the optimal shape for each particular state. This relaxation energy is found to be quite small (of the order of a few hundred reciprocal centimeters) except for the $^1A_{1g}(t_{2g}^6)$ state, where it amounts to ~5000 cm^{-1}. It should be noted that the $^1A_{1g}$ state is more stabilized by relaxation effects than by LFCI in the frozen orbital approximation (~2000 cm^{-1}). The reason why the $^1A_1$ state behaves anomalously is of course due to the fact that the frozen orbitals were calculated by an open-shell Hamiltonian, whereas the t_{2g}^6 state corresponds to a fully closed shell. For all other (open-shell) states, however, the effect of relaxation on the total energy differences is negligibly small—an observation that was found to be true also in other complexes.

As a consequence, the general features of the correlation diagram (Figures 1 and 2) are basically preserved, and a comparison between full-scale Hartree–Fock calculations and experiment is not significantly different from the discussion in the previous section. Therefore, the parameters B_{SCF}, C_{SCF}, and $10Dq_{SCF}$, shown in Table V, may be taken to describe also the complete Hartree–Fock calculations.[26]

(22) If only the first effect were operative, the d–d repulsion parameters would all be reduced by the same factor with respect to the atomic parameters. It would be unnecessary to use Griffith parameters: open-shell repulsion could adequately be described by a set of (reduced) Racah parameters.

(23) See also: Niyoshi, E.; Takada, T.; Obara, S.; Kashiwaghi, H.; Ohno, K. *Int. J. Quantum Chem.* **1981**, *19*, 451. In this work a semiempirical LFCI has been carried out for CoF_6^{3-}, on the basis of Hartree–Fock calculations, which are comparable to the present work.

(24) Janssen, G. J. M.; Nieuwpoort, W. C. *Philos. Mag. B* **1985**, *51*, 127.

(25) Daniel, C.; Hyla-Kryspin, I.; Demuynck, J.; Veillard, A. *Nouv. J. Chim.* **1985**, *9*, 581.

(26) Note the (small) discrepancy between $10Dq_{SCF}$ for $Co(CN)_6^{3-}$ in Table V (26 602 cm^{-1}) and the value listed in ref 17, where $10Dq_{SCF}$ is set equal to 27 978 cm^{-1}. In ref 17, $10Dq_{SCF}$ was obtained from a least-squares fit of the $t_2^6 \rightarrow t_2^5e^1$ transitions, whereas Table V equals $10Dq_{SCF}$ to the ($^5T_2 - {}^5E$) energy gap. The relatively small difference between both values is another indication of the adequacy of the ligand field parametrization scheme.

Table VII. Energy Differences between a Number of Different States Corresponding to a Given Configuration: $t_2^5e^1$ for $Co(CN)_6^{3-}$, $t_2^4e^2$ for CoF_6^{3-}, and d^6 for Co^{3+} [a]

			$\Delta E'$	$\Delta C_o'$	$\Delta C'$	$\Delta L'$	$\Delta T'$
$Co(CN)_6^{3-}$	$t_2^5e^1$	$^3T_{1g}$	0	0	0	0	0
		$^3T_{2g}$	8413	−16571	27050	−1926	−16667
		$^1T_{1g}$	7442	−20094	29451	−4218	−17800
		$^1T_{2g}$	23193	−62848	94583	−17951	−53441
CoF_6^{3-}	$t_2^4e^2$	$^5T_{2g}$	0	0	0	0	0
		^3E_g	31755	−25442	19886	52163	−40249
		$^3A_{2g}$	56621	−73627	50242	78374	−71995
Co^{3+}	d^6	^5D	0	0	0	0	0
		^3H	25988	13037	−39402	91384	−25995
		^3G	32833	16697	−48810	114476	−32833
		^1I	38921	19425	−59334	137181	−38926

[a] The results refer to ΔSCF calculations where a complete SCF calculation was carried out for each individual state. All energy differences (in cm^{-1}) are given with respect to the lowest state of the relevant configuration.

Table VIII. Behavior of the Different Energy Components of the Excited States in an Intraconfigurational Relaxation, If the Frozen Orbitals Correspond to the Lowest State of the Configuration[a]

C_o ↘	T_o ↘	L_o ↗
C_c ↗	T_c ↗	L_c ↘
C_{oc} ↘		

[a] C and T are always positive; L is negative. An increase of L therefore corresponds to a decrease of attraction stabilization.

2. Components of the Relaxation Energy. We will designate the SCF energy differences and its components by primed symbols, in order to stress the distinction with the frozen orbital calculations. Using the same notations as before, we have

$$\Delta E' = \Delta C' + \Delta L' + \Delta T' = \Delta C_o' + \Delta C_c' + \Delta C_{oc}' + \Delta L_o' + \Delta L_c' + \Delta T_o' + \Delta T_c'$$

The fact that $\Delta E' \simeq \Delta E$ does not prevent the relaxation from having rather important consequences for the energy components. Let us first consider the different states corresponding to one particular open shell, e.g. $t_{2g}^5e_g^1$ ($^3T_{1g}$, $^3T_{2g}$, $^1T_{1g}$, $^1T_{2g}$). The SCF energy differences and its components are shown in Table VII for a number of states corresponding to $t_{2g}^5e_g^1$ and $t_{2g}^4e_g^2$. For comparison, a few states of the parent atomic Co^{3+} ion are also shown. The most striking features of the table is the *negative* value of $\Delta C_o'$ in the molecular complexes, whereas the corresponding frozen orbital analogue $\Delta C_o = \Delta C = \Delta E$ is obviously positive. While the relative total energies are kept virtually unchanged, the relaxation process thoroughly modifies the interpretation of the excitation process. The details of this phenomenon are quite similar to what has been found in other transition-metal ions and complexes.[8,18,27,28] The nature of the relaxation process can most easily be understood by starting from an SCF calculation on the lowest state of the configuration under consideration. Using the frozen orbitals of this state, one can construct (very good) approximations to the total energy of the excited states belonging to the same configuration. If then the excited states are allowed to relax to their own SCF minimum (which is extremely close to the frozen orbital approximation) the different energy components change as shown in Table VIII. The open shell of the frozen excited state carries an undue amount of interelectronic repulsion, which it can decrease by expanding. As a consequence the open-shell components C_o, T_o and $|L_o|$ all decrease. The expansion of the valence shell entails a concomitant contraction of the metal core and an increase of the ligand-to-metal σ-donation. As a consequence C_c, T_c, and $|L_c|$ increase. The energy shifts of Table VIII have been found in all intraconfigurational relaxation phenomena studies so far. However, the dominant contributions may change from one case to another. In the $Co(CN)_6^{3-}$ and CoF_6^{3-} states of Table VII, for instance, $\Delta C'$ is positive, its sign being determined by $\Delta C_c'$ (the only positive component)—as opposed to $Cr(CN)_6^{3-}$ where $\Delta C'$ is negative[8] and the sign is determined by $\Delta C_{oc}'$. Similary, in all cases $\Delta C_o' < \Delta C_o$, but whether or not the expansion will be sufficiently important to make $\Delta C_o'$ negative depends on the specific case in question: it is in $Co(CN)_6^{3-}$ and CoF_6^{3-}, but it is not in Co^{3+} or $Cr(CN)_6^{3-}$ (Table VII).

A comparison of Hartree–Fock states belonging to *different* configurations lacks the simple guidelines offered by Table VIII and is generally more difficult to analyze. A case in point is the comparison of the singlet and quintet ground states of $Co(CN)_6^{3-}$ and CoF_6^{3-}, which are discussed in the next section.

Table IX. Energy Difference between the Lowest Singlet and the Lowest Quintet of Co^{3+}, CoF_6^{3-}, and $Co(CN)_6^{3-}$ As Determined from a ΔSCF Calculation: $\Delta E' = E'$(singlet) − E'(quintet)[a]

	Co^{3+}	CoF_6^{3-}	$Co(CN)_6^{3-}$
$\Delta E'$	38921	20586	−19919
$\Delta C'$	−59334	258896	370906
$\Delta L'$	137181	−91251	−64188
$\Delta T'$	−38926	−147059	−326637
E' ground state	−1379.447 07	−1977.973 63	−1934.883 42

[a] The total energies (bottom line) are in hartrees; the energy differences are in cm^{-1} (the Co^{3+} values were resumed from Table VII).

3. Comparison of the Hartree–Fock Ground States. Table IX shows the energy difference $\Delta E'$ and its components $\Delta C'$, $\Delta L'$, and $\Delta T'$ between the fully relaxed $^1A_{1g}(t_{2g}^6)$ and $^5T_{2g}(t_{2g}^4e_g^2)$ states of both complexes. Although the total energy differences $\Delta E'$ (Table IX) and ΔE (Table VI) are rather similar—as discussed in the previous sections—the energy components are again quite different, especially in the cyanide complex. It should be noted here that a further subdivision of $\Delta C'$ into $\Delta C_o' + \Delta C_c' + \Delta C_{oc}'$ is meaningless at the Hartree–Fock level where the $^1A_{1g}$ state has no open shells.

In both molecular complexes, $\Delta C'$ remains positive, showing that the $^1A_{1g}$ state carries more interelectron repulsion than the $^5T_{2g}$ state, thereby confirming the conventional description of the difference between singlet and quintet. This stands in marked contrast to the negative $\Delta C'$ value for the atomic Co^{3+} ion, where the ^1I state (parent state of $^1A_{1g}$) carries *less* repulsion than the ^5D ground state (parent center of $^5T_{2g}$). Obviously, this rather typical—but nonconventional—atomic behavior[8,18] is more than offset by the differential covalency of the dσ- and dπ orbitals.

Table IX also confirms the qualitative conclusion of the frozen orbital picture (Table VI) in that the quintet → singlet transition requires more repulsion for $Co(CN)_6^{3-}$ than for CoF_6^{3-}. This conclusion is the more remarkable as the $Co(CN)_6^{3-}$ orbitals are larger and more covalent, especially as the conventional spin-pairing energy ($5B_{SCF} + 8C_{SCF}$) is smaller for $Co(CN)_6^{3-}$ (Table VI).

VI. Conclusions

Hartree–Fock calculations do confirm the main conclusions that can be drawn from the classical Tanabe–Sugano correlation diagrams. They reproduce the correct ground states and the high-spin–low-spin transition between CoF_6^{3-} and $Co(CN)_6^{3-}$. The relative magnitude of the spectrochemical strength and the B and C parameters are qualitatively but not quantitatively reproduced for both complexes.

From a conceptual point of view, the Hartree–Fock calculations reveal a rather fascinating blend of corroborations and refutations of the ligand field picture.

For a strong field complex, Hartree–Fock calculations predict the interconfigurational gaps to be larger and the intraconfigurational gaps to be smaller than for a weak field complex—as expected from ligand field theory. But from a comparison of a set of isoconfigurational states, the open-shell repulsion is found to decrease with increasing energy, and from a comparison of a set of different configurations, the open-shell repulsion is found to decrease with increasing e_g population—both facts being in contradiction with ligand field theory.

(27) Vanquickenborne, L. G.; Hoet, P.; Pierloot, K. *Inorg. Chem.* **1986**, *25*, 4228.
(28) Vanquickenborne, L. G.; Pierloot, K.; Görller-Walrand, C. *Inorg. Chim. Acta* **1986**, *120*, 209.

Hartree–Fock calculations predict the correct order of magnitude for the spectrochemical strength, but the physical reason why $t_2^{m-1}e^{n+1}$ is higher than $t_2^m e^n$ has only an indirect relationship to the reason offered by ligand field theory. Hartree–Fock calculations corroborate the ligand field picture in associating a repulsion increase to the high-spin → low-spin transition, but the increase is predicted to be larger for the strong field complex—which contradicts the ligand field picture.

Apparently, ligand field theory (like atomic multiplet theory or Hund's rules) is better than the rationale upon which it has been built. The picture offered by Hartree–Fock calculations may be far from exact, but there are reasons to believe[27] that more reliable calculations (including electron correlation) will not affect the qualitative features of the model.

Registry No. CoF_6^{3+}, 15318-87-3; $Co(CN)_6^{3-}$, 14897-04-2.

Contribution from the Department of Chemistry,
North Dakota State University, Fargo, North Dakota 58105

Sharp Line Splittings in the Electronic Spectrum of Chloropentaamminechromium(III) Chloride

Kyu-Wang Lee and Patrick E. Hoggard*

Received September 1, 1987

A splitting of 16 cm^{-1} in the lowest energy spin-forbidden band has been observed in luminescence and excitation spectra of $[Cr(NH_3)_5Cl]Cl_2$. The two peaks have been assigned to the two components of the $^4A_{2g} \leftrightarrow {}^2E_g$ transition. Much larger ^2E_g splittings reported in the literature for this complex, and for the bromo and iodo analogues, have been reassigned to the splitting between the ^2E_g state and the lowest component of the $^2T_{1g}$ state. Ligand field calculations based on the exact ligand and counterion geometry yield a value of 1817 cm^{-1} for e_π of Cl^- and call into question earlier assumptions on the assignment of the spin-allowed transitions.

Introduction

Pentaammine complexes of chromium(III) and other metal ions have taken their places among the demonstration compounds of ligand field theory.[1-6] For d^3 and strong-field d^6 $[M(NH_3)_5X]^{n+}$ complexes the splitting of the first spin-allowed band is approximately equal to $(\Delta_N - \Delta_X)/4$, where Δ_N and Δ_X are the ligand field splitting parameters ($10Dq$) derived from the octahedral $[M(NH_3)_6]$ and $[MX_6]$ species.[1-7] Such correlations have been highly successful, as have those involving the second spin-allowed band of d^3 and d^6 complexes, although second-band splittings are less commonly observed experimentally.[8-10]

Splittings are also frequently observed among the three groups of sharp-line, spin-forbidden intraconfigurational transitions in d^3 complexes, $^4A_{2g} \rightarrow {}^2E_g$, $^2T_{1g}$, and $^2T_{2g}$ (in O_h notation). In particular, $^4A_{2g} \leftrightarrow {}^2E_g$ splittings have been reported for many Cr(III) complexes, because of the relative ease with which these lines can be detected in luminescence and absorption spectra. The pentaammine and tetraammine series were among the first to be investigated,[11-15] but the relatively large splittings observed (150–300 cm^{-1}) have long been a source of puzzlement. Ligand field theory, which works so well with the broad spin-allowed bands, appears to be incapable of generating splittings larger than 50 cm^{-1} for the pentaammines for any reasonable choice of parameters. Table I shows some representative literature values for the ^2E_g splitting in pentaammine complexes of Cr(III).

Table I. Reported ^2E_g Splittings for $[Cr(NH_3)_5X]^{n+}$ Complexes

X	splitting, cm^{-1}	anion	ref
Cl^-	170	ClO_4^-	14
	175	Cl^-	14
Br^-	225	Br^-	14
I^-	305	I^-	14
ONO^-	150	NO_3^-	14
	188	NO_3^-	13
H_2O	205	ClO_4^-	14
	87	NO_3^-	13
NCO^-	213	NO_3^-	16

The data for the halo pentaammines in Table I at least have some consistency. The ^2E_g splittings appear to increase with $\Delta_N - \Delta_X$. Ligand field theory predicts that the splitting of the first spin-allowed band depends on differences in $\Delta = 3e_\sigma - 4e_\pi$, where e_σ and e_π are the angular overlap model (AOM) destabilization parameters.[7] However, the splitting of the ^2E_g state has been shown to depend more on differences in $(e_\sigma + e_\pi)$ in AOM calculations.[17] Since Cl^-, Br^-, and I^- are stronger π-donors than NH_3 (which can be taken not to π-bond at all) and possibly weaker σ-donors, the sum $e_\sigma + e_\pi$ will be similar for NH_3 and the halides (except for F^-), even though $(3e_\sigma - 4e_\pi)$ values are quite different.

(1) Yamatera, H. *Bull. Chem. Soc. Jpn.* **1958**, *31*, 95.
(2) McClure, D. S. In *Advances in the Chemistry of the Coordination Compounds*; Kirschner, S., Ed.; Macmillan: New York, 1961; p 498.
(3) Wentworth, R. A. D.; Piper, T. S. *Inorg. Chem.* **1965**, *4*, 709.
(4) Wentworth, R. A. D.; Piper, T. S. *Inorg. Chem.* **1965**, *4*, 1524.
(5) Perumareddi, J. R. *J. Phys. Chem.* **1967**, *71*, 3155.
(6) Schläfer, H. L.; Gliemann, G. *Basic Principles of Ligands Field Theory*; Wiley-Interscience: London, 1969; Chapter 1.
(7) Schäffer, C. E.; Jørgensen, C. K. *Mat.-Fys. Medd.—K. Dan. Vidensk. Selsk.* **1965**, *34*(13).
(8) Glerup, J.; Mønsted, O.; Schäffer, C. E. *Inorg. Chem.* **1976**, *15*, 1399.
(9) Schläfer, H. L.; Martin, M.; Gausmann, H.; Schmidtke, H.-H. *Ber. Bunsen-Ges. Phys. Chem.* **1971**, *75*, 789.
(10) Decurtins, S.; Güdel, H. U.; Neuenschwander, K. *Inorg. Chem.* **1977**, *16*, 796.
(11) Porter, G. B.; Schläfer, H. L. *Ber. Bunsen-Ges. Phys. Chem.* **1967**, *68*, 316.
(12) Schläfer, H. L.; Martin, M.; Gausmann, H.; Schmidtke, H.-H. *Z. Phys. Chem.* (Munich) **1971**, *76*, 61.
(13) Shepard, W. N.; Forster, L. S. *Theor. Chim. Acta* **1971**, *21*, 135.
(14) Flint, C. D.; Matthews, A. P. *J. Chem. Soc., Faraday Trans. 2* **1973**, *69*, 419.
(15) Flint, C. D.; Matthews, A. P. *J. Chem. Soc., Faraday Trans. 2* **1977**, *73*, 655.
(16) Schönherr, T.; Schmidtke, H.-H. *Inorg. Chem.* **1979**, *18*, 2726.
(17) Hoggard, P. E. *Z. Naturforsch., A: Phys., Phys. Chem., Kosmophys.* **1981**, *36A*, 1276.

0020-1669/88/1327-0907$01.50/0